**Original Article**

# A New Method for Spatial Health Risk Assessment of Pollutants

*Mohamad Sakizadeh*[1], Hadi Ghorbani* [2]

*Received: 05.12.2016* *Accepted: 25.01.2017*


## ABSTRACT

**Background:** The area of contaminated lands exposed to the health risk of environmental pollutants is a matter of argument. In this study, a new method was developed to estimate the amount of area that is exposed to higher than normal levels of Cr, Mn, and V.

**Methods:** Overall, 170 soil samples were collected from the upper 10 cm of soil in an arid area in central part of Iran in Semnan Province. The values of Cr, Mn, and V were detected by ICP-OES technique. A geostatistical method known as sequential Gaussian co-simulation was applied to consider the spatial risk of these toxic elements.

**Results:** The moderate spatial dependence of Cr indicates the contribution of both intrinsic and extrinsic factor to the levels of this heavy metal in the study area, whereas, Mn and V can be attributed to intrinsic factors (such as lithology). There has not been any significant influence due to agricultural practices on the Cr values in the region. The surface of contaminated area for manganese, produced by risk curve on surface method, was higher than chromium and vanadium.

**Conclusion:** The produced risk curves as rendered in this study can be adopted in similar studies to help managers to estimate the total area that requires cleanup action.


**Keywords:** Heavy Metals, Risk Assessment, Risk Curve On Surface, Sequential Gaussian Co-Simulation.

**IJT 2017 (3): 39-45**





## INTRODUCTION

According to the environmental quality standards, heavy metals (HMs) can threaten the health of local residents (e.g. through consumption of contaminated plants) if their levels in soil exceed some threshold values. There have been multiple types of research on the monitoring of heavy metals in environmental media (e.g. soil, plants, sediments, etc.) in Iran and the world. For example, the distribution of HMs in some agricultural soils in Tehran [1]; the bioaccumulation of lead and manganese on some plant species in Semnan Province [2] and HM's accumulation in the sediments of Anzali Wetland [3].

In this field, one of the questions posed by environmental researchers is the area of contaminated land exposed to the health risk of environmental pollutants (e.g. HMs). The areas that need to be managed by managers are known, accordingly. These regions are usually located in regions in which the level of pollution exceeds the health risk standard levels. For instance, the problem of identification of rehabilitation area can be solved via simulations, through quantification of the risk of exceeding a significant threshold for each variable. In this way, rehabilitation strategies can simply be planned by decision makers and managers [4].

There have been multiple applications of sequential Gaussian co-simulation for the study of spatial pattern of soil attributes including soil organic matter [5], bioavailable parts of phosphorus and potassium [6], and soil salinity [7]. However, even though, there is few case studies about its application for the assessment of contaminated sites. For instance, used SGCS thereby risk assessment for contaminated sites by organic and inorganic pollutants in northern part of Italy [8].

The main objective of the current study was to develop a method, for the first time, to consider the spatial health risk assessment of heavy metals (Cr, Mn, and V) in an arid area, through different realizations produced by sequential Gaussian co-simulation method (SGCS) which is a geostatistical technique. Through implementation of this method, the area that needs to be

1. Department of Environmental Sciences, Shahid Rajaee Teacher Training University, Tehran, Iran.
2. Department of Soil Sciences, University of Shahrood, Shahrood, Iran.
*Corresponding Author: E-mail: msakizadeh@srttu.edu

rehabilitated is estimated easily. This study area was selected for the values of the above-mentioned HMs in soil samples exceeded the threshold standard levels in this region based on our monitoring program. Moreover, the spatial map of the contaminated areas will be produced by geostatistical methods as well.

## MATERIAL AND METHODS

### *Field, Laboratory Analysis, and Statistical Analysis*

The study region, with an area of 4416 $km^2$, is located in an arid area in which the main source of water for agricultural and household usage is provided through groundwater. Next, to agriculture, mining activity is the other source contributing to the contamination of soil and groundwater with HMs in recent years [9, 10].

A systematic random sampling was followed to collect 170 soil samples from the upper 10 cm of soil. In laboratory, the collected soil samples were air-dried and sieved through a 2-mm stainless steel mesh to remove stones and plant roots. The digestion of soil samples was implemented by a mixture of nitric acid ($HNO_3$) and hydrochloric acid (HCl) in a ratio of 3:1 ($HNO_3$: HCl). The digested samples were analyzed by inductively coupled plasma (ICP) optical emission spectroscopy (ICP-OES) to record the total concentrations of trace elements including Cr, Mn, and V. An illustrative map of the study is provided in Figure 1.To test the hypothesis about the possible role of agricultural activities on the soil's levels of Cr and Ni, a Mann-Whitney U-test was performed on the concentrations of Cr in agricultural fields against that of other land-uses.

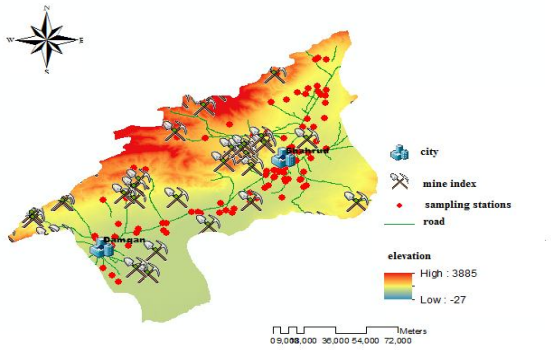


**Figure 1.** An illustrative map of the study area in which sampling stations have been highlighted.

### *Sequential Gaussian Co-Simulation*

Recently, multiple simulation methods such as Sequential Gaussian Simulation (SGS) [11], Turning Bands [12] and Simulated Annealing [13] have been utilized to obtain simulation maps of soil attributes; however, the most applied one is SGS [14]. In this method, a normal conditional cumulative distribution function is first determined for each value to be simulated at each simulation grid cell followed by sequential simulation of original data and the previously simulated values with neighborhood assigned based on the distance between sampling points. The data values approximately comply with normality assumption (otherwise the data have to be transformed to normal values using normal score transformation), SGS method use a variogram model and simple kriging to determine mean and variance of the Gaussian conditional cumulative distribution function (ccdf). This value is then inserted into the grid and added to the data. The process is then repeated by simulating the value of the next node in the grid until all of the nodes have been simulated [14].

On the contrary, in sequential Gaussian co-simulation (SGCS) [15], the principles of SGS and co-kriging are combined and simulation of the primary variable is conditioned to both primary and secondary data [16]. In the latest method, despite the SGS, variograms, and cross-variograms should be fitted with a linear model of coregionalization (LMC) to satisfy the positive definiteness condition [17]. In this technique, simple collocated cokriging is used instead of simple kriging to implement the simulations [5] and the conditioning data consists of primary and secondary data along with the previously simulated values. In both SGS and SGCS, the simulated values are back-transformed using the inverse of the Gaussian anamorphosis function used for normal score transformation of original data.

### *Spatial Health Risk Assessment*

Independent paths were utilized to perform 1000 different SGCS realizations on a simulation grid of 1000m×1000m using normal score transformed values of Cr, Mn, and V resulting in $\ell$ equiprobable realizations. In this single-location uncertainty method [18], these realizations can subsequently be used to calculate the probability that the unknown HMs ($z(x')$) at location $x'$,

exceed given thresholds value ($z_t$), denoted as $\mathbf{Prob[z(x') > z_t]}$ and it is being calculated as follows:

$$\mathbf{Prob[z(x') > z_t] = \frac{n(x')}{1000}} \quad (1)$$

Where $\mathbf{n(x')}$ represents the number of realizations (out of 1000 realizations) in which the concentration values was greater than the threshold (e.g. standard level for HMs in this case). To calculate the spatial health risk of these HMs we produce curves, called risk curve on surface. The number of nodes for which the respective HM was equal or higher than the cutoff value was calculated first using 1000 generated realizations and the results were multiplied by the unit surface of the simulation grid to obtain the risk curve on surface for each HM. Three different quantiles (including 5, 50 and 95) were applied to report the spatial risk of calculations. The standard values for Cr, Mn, and V were 110600 and 100mg/kg, respectively.

## RESULTS

The histograms of investigated heavy metals (Cr, Mn, and V), indicting the frequency distribution each element, have been depicted in Figure 2. On the other hand, Figure 3 illustrates the variogram model fitted to each HM while the respective variogram parameters were rendered in Table 1. The results of variogram model fitting (Figure 3) showed that the best-fitted model for Mn and V was a spherical model whereas an exponential model better fitted to the experimental vatiogram of Cr. The mean of simulated Cr, Mn and V using SGCS (also known as E-Type map) is depicted in Figure 4. On the contrary, the resultant Mann-Whitney U-test did not produce any significant result indicating that agricultural practices have not significantly influenced the values of Cr in the study area or they have not used Cr as impurities in their applied fertilizers.

The results of risk curves on surface are depicted in Figure 5, for Cr, Mn, and V, respectively. The surface area ($Km^2$) for which the simulated value of Cr has been equal or greater than the guideline level fluctuated between 481 $km^2$ and 1214 $km^2$ with an average value of 782.39 $km^2$. Nearly 18% of the study area had chromium levels that were equal to or greater than the standard level of 110 mg/kg. The critical quantiles of 5, 50 and 95 were also obtained 616 $km^2$, 778 $km^2$ and 971 $km^2$ indicating the uncertainty of our calculations. Referring to risk curve on surface of Mn, the simulation's predictions varied between 1710 $km^2$ and 2781 $km^2$ with an average value of 2230.09 $km^2$, meaning that 50% of the total study area have manganese values equal to or greater than the standard level of 600mg/kg. The predictions were also 1928, 2230 and 2520 $km^2$ for 5, 50 and 95 quantiles, respectively.

**Table 1.** Parameters of variogram models for each HM.

| Heavy metals | Variogram model | $C_0$ $(mg/kg)^2$ | $C+C_0$ $(mg/kg)^2$ | $C_0/C+C_0$ | Range (km) |
|---|---|---|---|---|---|
| Cr | Exponential | 173.20 | 499.80 | 0.35 | 23.71 |
| Mn | Spherical | 700.00 | 34900 | 0.02 | 7.19 |
| V | Spherical | 78.54 | 499.90 | 0.16 | 29.85 |

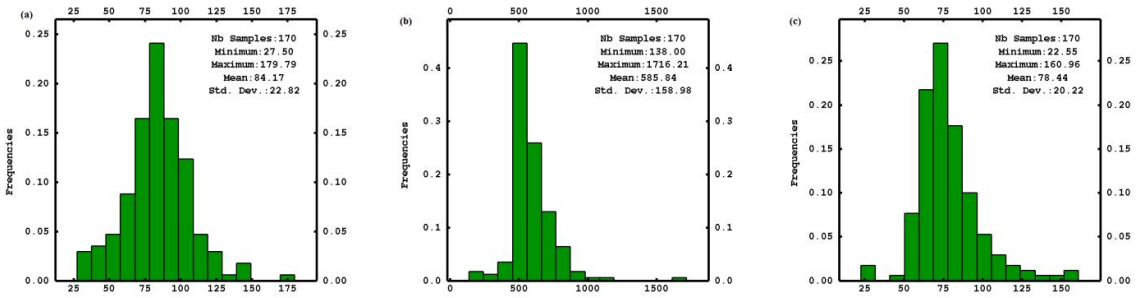


**Figure 2.**Histogram of a (Cr),b(Mn) and c(V).

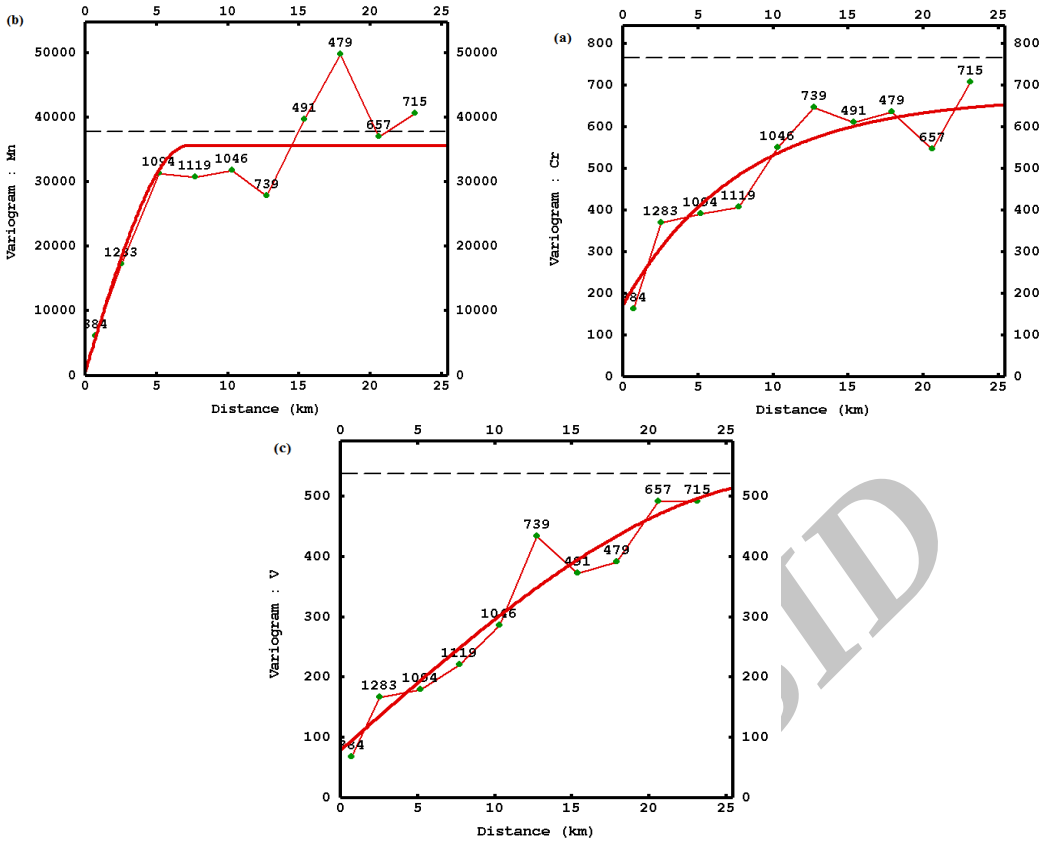


**Figure 3.**Variogram models fitted to experimental variogram of each HM.

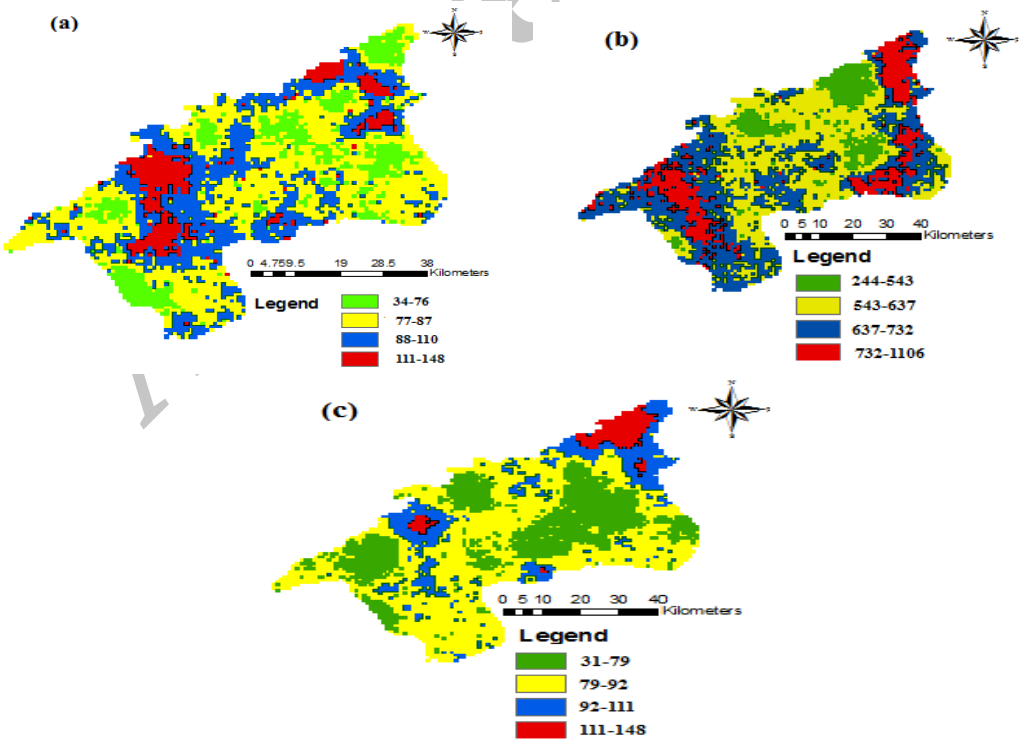


**Figure 4.** Produced map related to mean of realizations for a (Cr), b (Mn) and c (V).

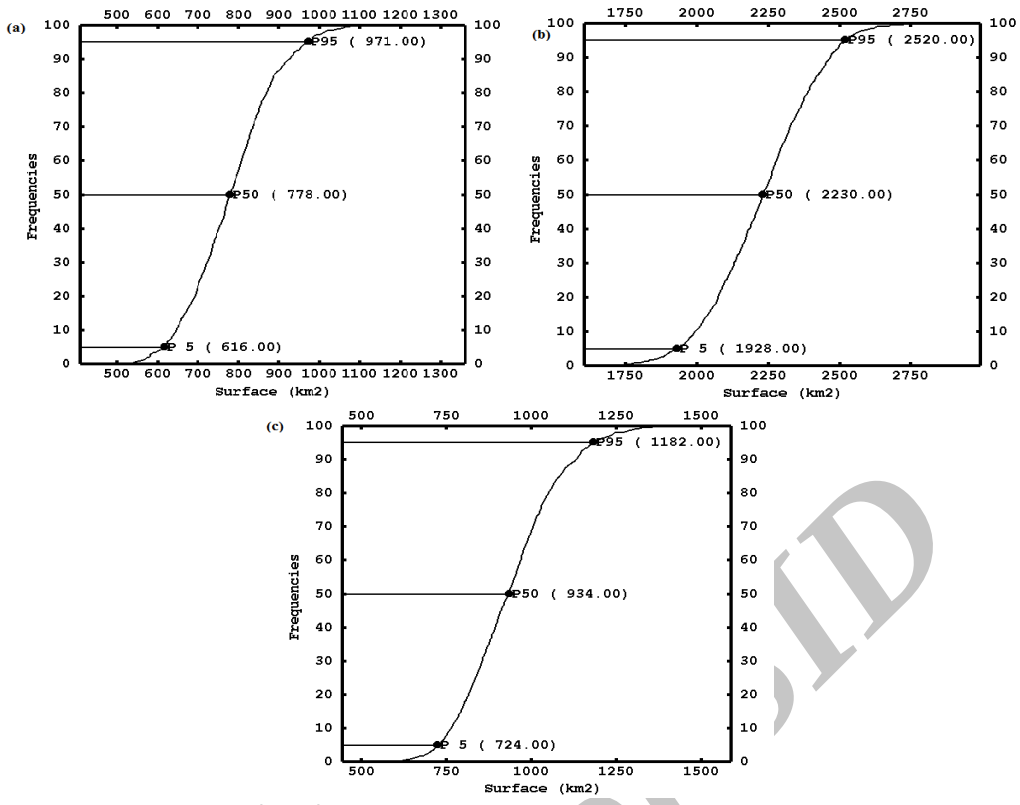


**Figure 5.** Risk curve on surface for a(Cr),b(Mn),c(V) and the respective 5, 50 and 95 probabilities.

The generated risk curve on surface for V shows a higher risk than Mn but a lower risk than that of Cr. The area equal or higher than the cutoff value, in this case, ranged between 432 $km^2$ and 1412 $km^2$ with a mean value of 938.30$Km^2$ indicating that about 21% of the total study area might have been contaminated. The respective levels of 5, 50 and 95 quantiles were 724934 and 1182 $km^2$, respectively.

## DISCUSSION

Among 170 soil samples, 18 samples for Cr (10.6%), 21 samples for V (12.4%) and 57 samples for Mn (33.5%) had exceeded the related standard values of 110 mg/kg, 100 mg/kg and 600 mg/kg, respectively.

Nugget to sill ratio (Table 1) can be used to consider the extent of intrinsic (such as geological formations and soil parent material) or extrinsic factors (e.g. agricultural, urban or industrial activities) on the spatial variability of soil properties [11]. Values less than 25% indicate strong spatial dependent and can be attributed to intrinsic factors while levels between 25% and 75% implying moderate spatial dependent and are attributable to both intrinsic and extrinsic factors [19]. The spatial variability of Mn and V are strong while Cr are moderate indicating the contribution of both soil parent materials and anthropogenic sources (e.g. mining and agricultural activities in this case) to the measured values of chromium in soil samples (Table 1).

The mean realization has been categorized into four quantiles considering the lowest and highest contamination level in each map. There are some localized hotspots associated with each HM highlighted using red colors. Referring to spatial variability of each these HMs, the moderate spatial dependence of Cr indicates the contribution of both intrinsic and extrinsic factor to the levels of this HM, Mn, and V can be attributed to intrinsic factors (such as lithology). The elevated levels of Cr have been proved to emanate from the ultramafic rocks and the resultant soils developed due to the weathering of these geological facies [20]. The association between the elevated levels of Cr and ultramafic parent materials (e.g. serpentinite) has been well documented in other published literature as well [21; 22]. The higher than standard values of chromium (e.g. up to 179.8$mgkg^{-1}$) in some soil samples might be due to the prevalence of these soils in some parts of the study area [23]. This confirms the possible contribution of parent

materials to the values of chromium. However, even though, there is some localized contamination related to Cr in southwest and northeastern part of the region. The southwest part's hotspot coincided with some mining activities based on the land use map (Figure 1). At least in some parts of the region, the elevated levels of Cr can be attributed to prevalent mining activities. Pyrite oxidation at waste dump in mining area caused pick concentration of sulfate [24]. The elevated levels of some HMs (including Cr) in the nearby of mining area have originated from these activities [25]. On the other hand, Cr is available in appreciable amounts as impurities in phosphate fertilizers [26].

The levels of Mn in soils are very different, however; soils derived from mafic rocks and soils in arid and semi-arid regions (like the study area) usually contain elevated levels of this element [27]. This may partly justify the high-detected levels of this heavy metal in some parts of the region. Moreover, oil exploration next to parent materials and pedogenic processes happening during soil development are main sources of vanadium in soil samples. The absence of oil exploration operation in the study area attests to the results of variography implying that vanadium and manganese have most probably emanated from soil formation factors and parent materials.

Given the uncertainty of predictions made by risk curve of surface results, the uncertainty of predictions of manganese was roughly lower than chromium that might be due to the local impacts of anthropogenic sources resulting in more patchy hotspots than intrinsic source. The produced risk curves as rendered in this study can be adopted in similar studies to measure the reliability of contaminated area and help managers to estimate the total area that requires cleanup action. In cases that researchers have the required budget to collect 3D samples (e.g. not only on the surface but also in the deeper parts of the soil), the risk curve on volume can also be obtained indicating the total amount of contaminated soil. In this way, the amount of budget needed to remediate the contaminated soil (in situ or off site) can be estimated as well.

## CONCLUSION

A method that called risk curve on surface was proposed to account for the spatial risk of HMs through risk curve of surface plots. Using these curves, the quantiles of areas for which the level of contamination is equal or higher than the standard values can be calculated thereby an estimate of spatial risk is provided for researchers. These curves measure the reliability of delineating contaminated area and help managers to plan for the future cleanup actions.

## ACKNOWLEDGEMENT

This work was supported by Shahid Rajaee Teacher Training University under contract number 29716. The authors are also grateful to the help of Geological survey of Iran to fulfill the goals of this study.

## REFERENCES

1. Rezaeian M, Moghadam MT. Determination of Heavy Metal in Agricultural Soils near and Far From the Cement Factory in Tehran, Iran. Iran J Toxicol 2016;10(5):23-6.
2. Sakizadeh M, Mirzaei R, Ghorbani H. Accumulation and Soil-to-Plant Transfer Factor of Lead and Manganese in some Plant Species in Semnan Province, Central Iran. Iran J Toxicol 2016;10(3):29-33.
3. Ganjali S, Ghasemi A. Heavy Metal Contamination in the Sediments of Anzali International Wetland, Northern Iran Based on Type Regional Development. Iran J Toxicol 2016;10(5):1-6.
4. De-Vitry C, Vann J, Arvidson H, editors. A guide to selecting the optimal method of resource estimation for multivariate iron ore deposits. Proceedings of the Iron Ore Conference; 2007: Citeseer.
5. Chai X, Huang Y, Yuan X. Accuracy and uncertainty of spatial patterns of soil organic matter. New Zeal J Agr Res 2007;50(5):1141-8.
6. Larocque G, Dutilleul P, Pelletier B, Fyles JW. Conditional Gaussian co-simulation of regionalized components of soil variation. Geoderma 2006;134(1):1-16.
7. Yao R, Yang J, Shao H. Accuracy and uncertainty assessment on geostatistical simulation of soil salinity in a coastal farmland using auxiliary variable. Environ Monit Assess 2013;185(6):5151-64.
8. Guastaldi E, Del Frate AA. Risk analysis for remediation of contaminated sites: the geostatistical approach. Environ Earth Sci 2012;65(3):897-916.
9. Sakizadeh M, Mirzaei R, Ghorbani H. The Extent and Prediction of Heavy Metal Pollution in Soils of Shahrood and Damghan, Iran. Bull Environ Contam Toxicol 2015;95(6):770-6.

10. Sakizadeh M, Mirzaei R, Ghorbani H. Support vector machine and artificial neural network to model soil pollution: a case study in Semnan Province, Iran. Neural Comput Applic 2016; 3:1-10.
11. Lin W-C, Lin Y-P, Wang Y-C. A decision-making approach for delineating sites which are potentially contaminated by heavy metals via joint simulation. Environ Pollut 2016;211:98-110.
12. Raco B, Dotsika E, Battaglini R, Bulleri E, Doveri M, Papakostantinou K. A quick and reliable method to detect and quantify contamination from MSW landfills: a case study. Water Air Soil Pollut 2013;224(3):1380-1.
13. Barca E, Castrignanò A, Buttafuoco G, De Benedetto D, Passarella G. Integration of electromagnetic induction sensor data in soil sampling scheme optimization using simulated annealing. Environ Monit Assess 2015;187(7):422-33.
14. Webster R, Oliver MA. Geostatistics for environmental scientists: John Wiley & Sons; 2007.
15. Verly G. Sequential Gaussian cosimulation: a simulation method integrating several types of information. Geostatistics Troia'92: Springer; 1993. p. 543-54.
16. Hohn ME. Geostatistics and Petroleum Geology. Kluwer Academic Publishers; 1999.
17. Clayton D, André J. GSLIB-Geostatistical software library and user's guide. Technometrics; 1998.
18. Goovaerts P. Geostatistical modelling of uncertainty in soil science. Geoderma 2001;103(1):3-26.
19. Liu X, Xu J, Zhang M, Zhou B. Effects of land management change on spatial variability of organic matter and nutrients in paddy field: a case study of Pinghu, China. Environ Manag 2004;34(5):691-700.
20. Kelepertsis A, Alexakis D, Kita I. Environmental geochemistry of soils and waters of Susaki area, Korinthos, Greece. Environ Geochem Hlth 2001;23(2):117-35.
21. Shewry P, Peterson P. Distribution of chromium and nickel in plants and soil from serpentine and other sites. J Eol 1976:195-212.
22. Alloway BJ. Heavy Metals in Soils: Trace Metals and Metalloids in Soils and their bioavailability; 2012.
23. Namaghi HH, Karami GH, Saadat S. A study on chemical properties of groundwater and soil in ophiolitic rocks in Firuzabad, east of Shahrood, Iran: with emphasis to heavy metal contamination. Environ Monit Assess 2011;174(1-4):573-83.
24. Ardejani FD, Shokri BJ, Moradzadeh A, Soleimani E, Jafari MA. A combined mathematical geophysical model for prediction of pyrite oxidation and pollutant leaching associated with a coal washing waste dump. Int J Environ Sci Tech 2008;5(4):517-26.
25. Doulati Ardejani F, Jodieri Shokri B, Moradzadeh A, Shafaei SZ, Kakaei R. Geochemical characterisation of pyrite oxidation and environmental problems related to release and transport of metals from a coal washing low-grade waste dump, Shahrood, northeast Iran. Environ Monit Assess 2011;183(1):41-55.
26. Mermut A, Jain J, Song L, Kerrich R, Kozak L, Jana S. Trace element concentrations of selected soils and fertilizers in Saskatchewan, Canada. J Environ Qual 1996;25(4):845-53.
27. Kabata-Pendias A, Mukherjee AB. Trace elements from soil to human: Springer Science & Business Media; 2007.